



Effects of Shallow Saline Groundwater Table Depth and Evaporative Flux on Soil Salinity Dynamics using Hydrus-1D

Bhaskar Narjary¹ · Satyendra Kumar¹ · Murli Dhar Meena^{1,2} · S. K. Kamra¹ · D. K. Sharma¹

Received: 18 April 2020 / Accepted: 29 August 2020 / Published online: 5 November 2020
© NAAS (National Academy of Agricultural Sciences) 2020

Abstract Soil salinization is a major environmental problem and critical concern in arid and semiarid regions. Hydrus-1D model was used to simulate effects of shallow saline groundwater table depth and evaporative flux on soil salinity movement in a saline environment. After successful calibration and validation with recorded soil moisture and soil salinity data, the model was used to evaluate two hypothetical scenarios for managing soil salinity, i.e., with 5 groundwater table depths (WTD) (WTD as on 2015, 25% and 50% rise; 25% and 50% decline in WTD based on the 2015 reference depth) and 3 different evaporative flux conditions (25, 50 and 75% reduction in evaporative flux). The model was calibrated, validated and run for scenarios with 2015 weather and WTD condition for the periods of 288 days. During calibration periods, root mean square error (*RMSE*) value of soil moisture content was $0.023 \text{ cm}^3 \text{ cm}^{-3}$ and for soil salinity was 2.58 dS m^{-1} , while during validation period *RMSE* of $0.023 \text{ cm}^3 \text{ cm}^{-3}$ and 1.5 dS m^{-1} , respectively, was recorded for soil moisture and soil salinity. Simulation results indicated that summer season (March to May, 60–150 Julian days) is the most important time to control soil salinity in this region. Considerable upward salt movement occurred during this period with 25 and 50% rise in groundwater table depth. Average root zone soil salinity increased by 6 and 12 dS m^{-1} when WTD raised by 25 and 50%, respectively, but negligible change in soil salinity was observed when groundwater table declined by 25 and 50%. The effective way to control this upward salt movement was reducing evaporative demands. Simulation study indicated that reducing evaporative flux of 25, 50 and 75% reduced profile soil salinity by 3.53, 6.95 and 12.38 dS m^{-1} , respectively, during peak summer period.

Keywords Soil salinity · Shallow saline groundwater · Hydrus 1-D · Evaporative flux

Introduction

Rapid development of irrigation infrastructure without considering optimum implementation of drainage measures has caused rise in the groundwater table and consequent widespread waterlogging and salinization in several arid and semiarid regions in the World [26]. Waterlogging, soil and groundwater salinity are serious environmental

impediments which adversely affect the crop yield, soil health and socioeconomic well-being of the farming community. In India, nearly 6.73 million (M) ha area is occupied by salt-affected soils out of which saline soils occupy 2.96 M ha, including 1.75 M ha of inland salinity [14]. Soil salinity threatens the sustainability of irrigated agriculture, particularly in arid and semiarid agro-climatic region by limiting its crop productivity and land degradation. [4, 15]. Management of this degraded land includes appropriate soil and water management practices, groundwater table management and reduced evaporative fluxes [19, 20, 22] through mulch in the soil surface or cover crops [1, 5, 17].

In an arid and semiarid climate where rainfall is very limited, shallow saline groundwater plays an important role

✉ Bhaskar Narjary
bhaskar.narjary@icar.gov.in

¹ ICAR-Central Soil Salinity Research Institute, Karnal, India

² Present Address: ICAR-Directorate of Rapeseed and Mustard Research, Bharatpur, India

in ecosystem functions [31]. Due to non-availability of freshwater, farmers of this region often compelled to use underneath shallow saline groundwater for irrigation [30]. Therefore, it is very much important to know the effects of the groundwater table depth (WTD) and groundwater salinity on root zone salt and water movement and salinity buildup. The spatiotemporal variation of the groundwater table depth and its quality is the major process for the exchange of salt between the vadose zone and the groundwater system. The rise of groundwater table is one of the main key factors responsible for soil salinization over large areas, as rising groundwater carries salt from deep soil layers to the surface through evaporative upward flux [29]. The salt balance in the root zone depends upon the land use and management practices, such as irrigation and cover crops.

Several factors affecting the salt and water movement in shallow groundwater condition and their interactions are also complex. Evaluation of these factor and their interactions in field is time-consuming and labor intensive. Moreover, in a single growth season, these changes in salt variation are often minute and non-detectable. Water and solute transport modeling plays a significant role in the understanding the process of soil salinization, in particular upward and downward movement, and in devising strategies for salinity control. Water and solute transport model, mainly solved through numerical solution, once calibrated with observed data, can be used to simulate water and solute transport in large areas. Transport modeling is particularly useful in the development of salinization scenarios for given climate and groundwater conditions and management practices.

In this study, Hydrus-1D model, which simulates one-dimensional transport of water, heat and solutes in variably saturated and unsaturated media, was adopted to simulate the soil water and salt transport in shallow saline groundwater condition of semiarid climatic region. From the perspective of salinization dynamics, we were interested in [1] to test the feasibility of the Hydrus-1D model approach in simulating water flow and salt transport with observed data; [2] to conduct scenario analyses for the soil water and salt dynamics under different WTD and evaporative conditions.

Materials and Methods

Study Area, Evaporation and Rainfall Distribution

The study was conducted at experimental farm of Central Soil Salinity Research Institute, Karnal, which is located near to Nain village in Panipat district of Haryana, India. The farm is of 11 ha size and extends geographically between

29°19′7.09″ to 29°19′10″N latitude and 76°47′30.0″ to 76°48′0.0″E longitude and at an elevation of 230–235 m above mean sea level (Fig. 1). About 77% of mean annual rainfall of 550 mm occurs during southwest monsoon season, while the annual evaporation is about 1500 mm. The area comes under the *Ustic* soil moisture regime [13] and had been lying abandoned for 20 years due to high salinity and presence of a shallow saline water table [16]. Soil is characterized by a sandy loam in texture, and according to USDA (United States Department of Agriculture), soil taxonomy is classified as mixed typic haplustepts (saline phase) [13]. The land has been abandoned for nearly two decades and more than half of the farm area (55.4%) has been mapped as severely saline (16–32 dS m⁻¹) with a smaller area (6.3%) being extremely saline (> 32 dS m⁻¹) [16].

Total rainfall received during 2015 was 1003 mm of which 814 mm was received during monsoon months (Fig. 2). This was exceptionally high in this region as compared to average rainfall. During monsoon months, two high-intensity rainfall events of 185 and 125 mm occurred on 194 and 224 Julian days, respectively. Daily pan evaporation ranged from 8 to 12 mm during the summer months (April to June) and 1 to 7 mm during winter (Jan–March) months (Fig. 2).

Soil Moisture, Salinity and Groundwater Observations

Soil samples were collected at regular interval from soil layers of 0–15, 15–30, 30–60 and 60–90 cm deep using a screw auger for gravimetric determination of soil moisture content (SMC) during the period from 7 to 288 Julian days of 2015. Gravimetrically measured SMC ($w w^{-1}$) was converted to volumetric SMC ($v v^{-1}$) percentage by multiplying with bulk density. Soil salinity of the soil saturation extract (EC_e) was measured using electrical conductivity meter. Since soil salinity in Hydrus-1D is expressed as electrical conductivity of soil solution (EC_{sw}), EC_e values were converted into EC_{sw} by Eq. 1

$$EC_{sw} = EC_e \frac{\theta_s}{\theta_t}, \quad (1)$$

where θ_s is the saturated soil moisture content ($L^3 L^{-3}$) and θ_t is the soil moisture content ($L^3 L^{-3}$) at the time of observation.

Observation wells had been installed for regular monitoring of water table fluctuations. Water level recorder (OTT KL 010, OTT Hydromet) was used to measure water table depth and water sample collecting device was used to collect water samples from installed observation well. Groundwater salinity (EC_{gw}) was determined using a standard electrical conductivity meter (Eutech Con 700, Eutech Instruments Pvt Ltd, Singapore).

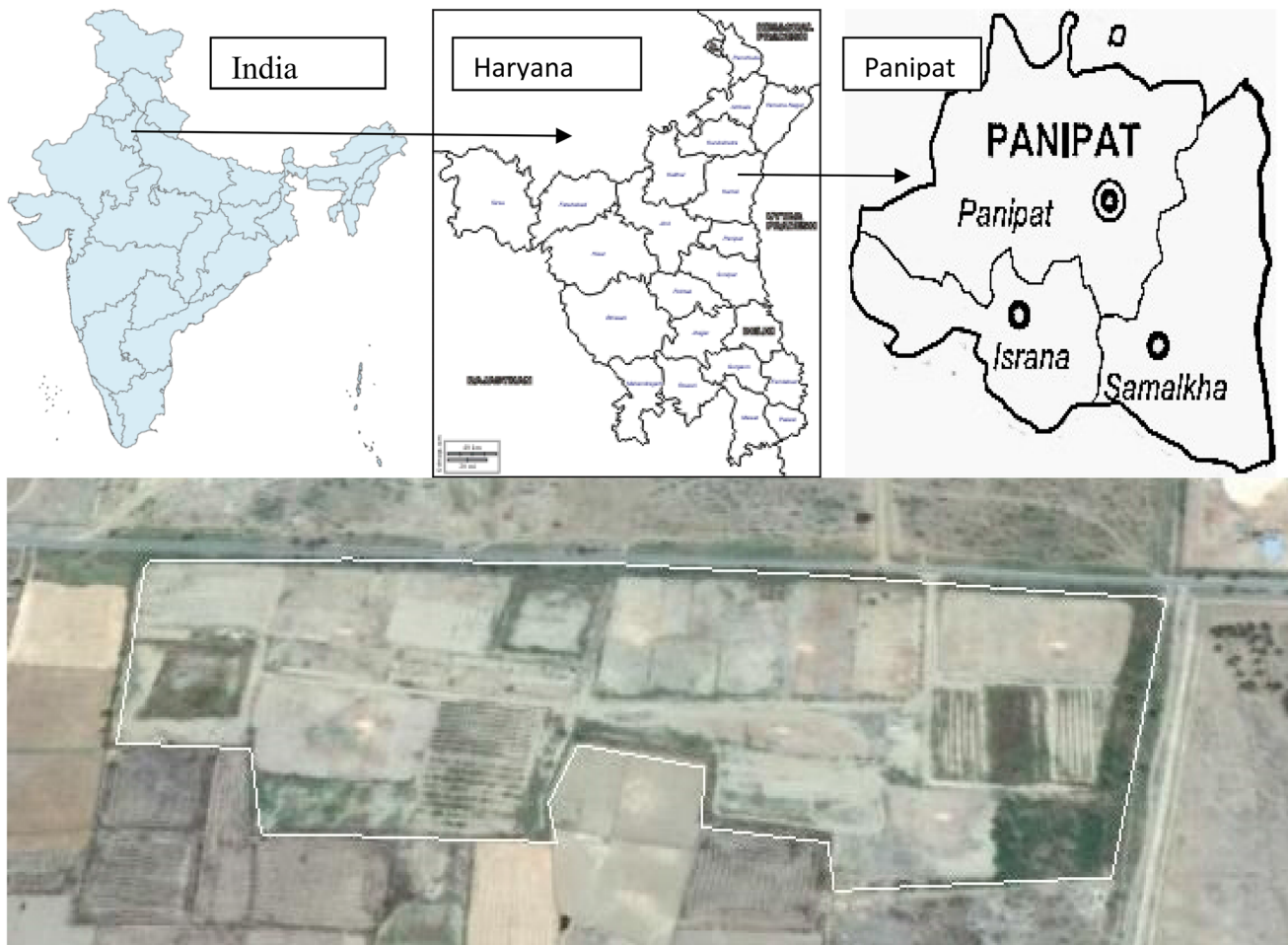
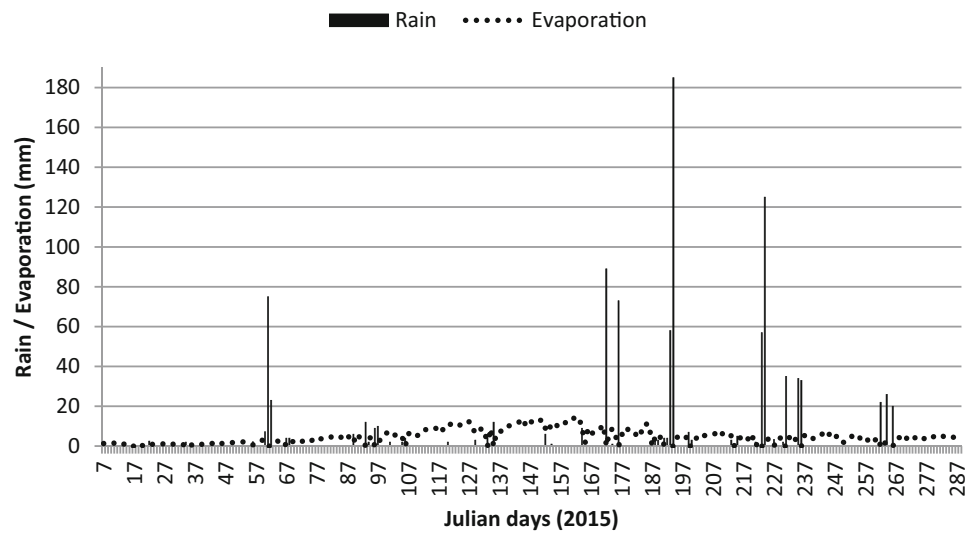


Fig. 1 Location map of experimental farm (Nain, Panipat, Haryana, India)

Fig. 2 Daily rainfall and evaporation during the simulation period 2015



Model Description

Simulations of soil moisture flow and salt transport were performed with Hydrus-1D. Hydrus-1D numerically solves

the Richard’s equation for moisture movement and advection–dispersion equation for salt transport in variably saturated porous media. Richard’s equation was used to describe the soil moisture flow using Eq. 2

$$\frac{\delta\theta}{\delta t} = \frac{\delta}{\delta z} \left[K \left(\frac{\delta\theta}{\delta h} + 1 \right) \right] - S[z, t]. \quad (2)$$

The soil water retention [θ (h)] and hydraulic conductivity [K (h)] relationships in Eq. [2] were described using van Genuchten–Mualem [24] functions as follows

$$\theta = \begin{cases} \theta_r + \frac{\theta_s - \theta_r}{(1 + |\alpha h|^n)^m} & h < 0 \\ \theta_s & h \leq 0 \end{cases} \quad (3)$$

$$K(h) = K_s S_e^l \left[1 - (1 - S_e^{1/m})^2 \right], \quad (4)$$

where θ_r and θ_s are the residual and saturated water contents ($L^3 L^{-3}$), respectively, which were determined by pressure plate apparatus (Soil moisture equipment, California, USA), K_s ($L T^{-1}$) is the saturated hydraulic conductivity, α [L^{-1}] and n represent the empirical shape parameters, $m = 1 + 1/n$, and ι is a pore connectivity parameter.

S_e is the effective saturation, given by Eq. 5:

$$S_e = \frac{\theta - \theta_r}{\theta - \theta_s}. \quad (5)$$

The partial differential equation governing transient one-dimensional salt movement in variably saturated medium is defined Eq. 6

$$\frac{\delta\theta C}{\delta t} = \frac{\delta}{\delta z} \left(\theta D \frac{\delta C}{\delta z} \right) - \frac{\delta v \theta C}{\delta z}, \quad (6)$$

where C is the solute (salt) concentration [ML^{-3}], D is the effective dispersion coefficient ($L^2 T^{-1}$) and v is the average pore water velocity (LT^{-1}). D is described by the following equation:

$$D = \lambda v, \quad (7)$$

where λ represents the longitudinal dispersivity [L].

Model Boundary Conditions

Atmospheric boundary condition with surface layer of 7 cm, representing possibility of maintaining 7 cm water head in the field with bund dykes, was selected as the upper boundary condition. Daily data of precipitation and evaporation were given as an input parameter for upper atmospheric boundary condition. Measured initial soil water content and soil solution salinity of various soil layers in the flow domain were used as initial conditions for simulating water and salt movement. For representing shallow saline groundwater condition at the bottom, variable pressure head and concentration were specified as bottom boundary conditions for water flow and salt transport using

the measured water table depths and groundwater salinity, respectively.

Model Parameterization

The model was calibrated with volumetric moisture content and the soil solution salinity (EC_{sw}) measured from 0–15, 15–30 30–60 to 60–90 cm soil profiles. The soil hydraulic properties of residual (θ_r) and saturated water contents (θ_s) were determined in the laboratory using pressure plate apparatus. Initial value of saturated hydraulic conductivity (K_s) and other van Genuchten–Mualem parameters, i.e., α , n and ι were estimated via Rosetta pedo-transfer functions using the particle size distribution and bulk density dataset [11]. The final Genuchten–Mualem parameters were optimized using Levenberg–Marquardt method of inverse analysis incorporated in the Hydrus-1D [24]. The dispersivity (λ) of different soil profiles was set by using trial and error. The calibrated soil hydraulic parameters are shown in Table 1. The coefficients of determination (r^2) and root mean square error (RMSE) were used to compare level of agreement between model-predicted and field-observed data.

Management Strategies Analysis

After validating the Hydrus-1D model, two management strategies were simulated for controlling soil salinity. The focus was to identify groundwater table depth for controlling soil salinity so that further salinization not occurs. To achieve this, we analyzed the effects of groundwater table depth on the soil water and salt balance. Taking the data of 2015 as the reference level, four WTD (i.e., WTD as on 2015, 25% and 50% rise in WTD; 25% and 50% decline in WTD based on the 2015 reference depth) were assumed in this process. Since in soil, salts transported upward through capillarity, therefore effects of evaporative demand on salt movement were also simulated as second strategy. For this, soil salinity was simulated under 25, 50 and 75% reduction in soil evaporation demand.

Results and Discussion

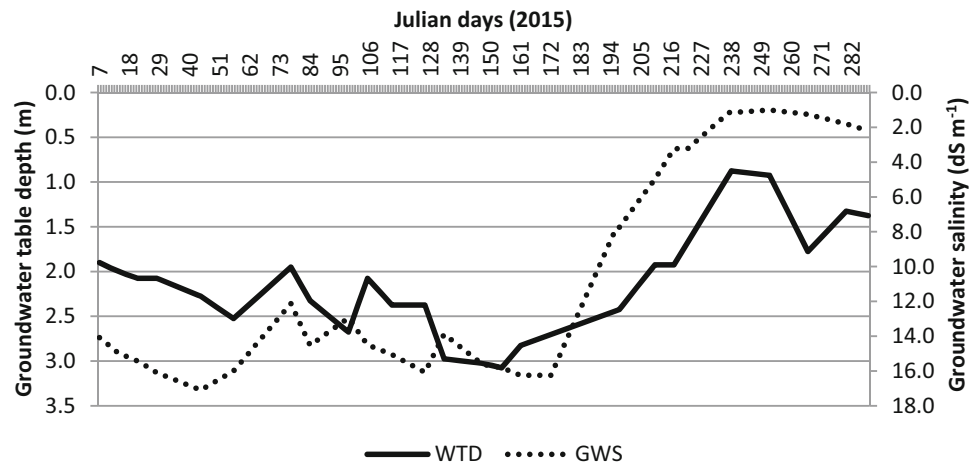
Groundwater Dynamics

The temporal variations in groundwater depth and salinity are presented in Fig. 3. During the study period, the groundwater depth ranged from 0.87 to 3 m below ground level (bgl) and groundwater salinity was ranged from 1 to 17.1 $dS m^{-1}$. In summer season (90–150 Julian days, 2015), groundwater table depth declined to 3 m bgl with groundwater salinity of 17 $dS m^{-1}$. During monsoon

Table 1 Soil physical properties and calibrated parameters at the study area

	0–15 cm	15–30 cm	30–60 cm	60–300 cm
Sand (%)	55.2	54.9	53.8	53.7
Silt (%)	29.6	28.3	29.2	28.6
Clay (%)	15.3	16.8	17.0	17.7
Bulk density(g cm^{-3})	1.5	1.6	1.6	1.6
θ_r ($\text{cm}^3 \text{cm}^{-3}$)	0.05	0.04	0.05	0.05
θ_s ($\text{cm}^3 \text{cm}^{-3}$)	0.4	0.4	0.4	0.4
α (cm^{-1})	0.004	0.004	0.005	0.008
n	2.1	1.9	1.5	1.4
K_s (cm d^{-1})	8.0	25.0	15.0	8.0
l	0.5	0.5	0.5	0.5
λ (cm)	4.9	17.6	14.1	29.8

Note The particle size limits were 0.05 to 2 mm for sand, 0.05–0.002 mm for silt and < 0.002 mm for clay. θ_r , residual water content; θ_s , saturated water content; α , reciprocal value of air entry pressure; n , the smoothness of pore size distribution; l , pore connectivity parameter; K_s , saturated hydraulic conductivity; and λ , dispersivity

Fig. 3 Groundwater table depth (m) and groundwater salinity (dS m^{-1}) during the simulation period 2015

period (172–246 Julian days, 2015) rising trend in groundwater depth and a decreasing trend in salinity were observed. High-intensity rainfall of 18.5 cm on 194 Julian days probably brought down the groundwater salinity from 11 to 7.7 dS m^{-1} through dilution.

Model Calibration and Validation

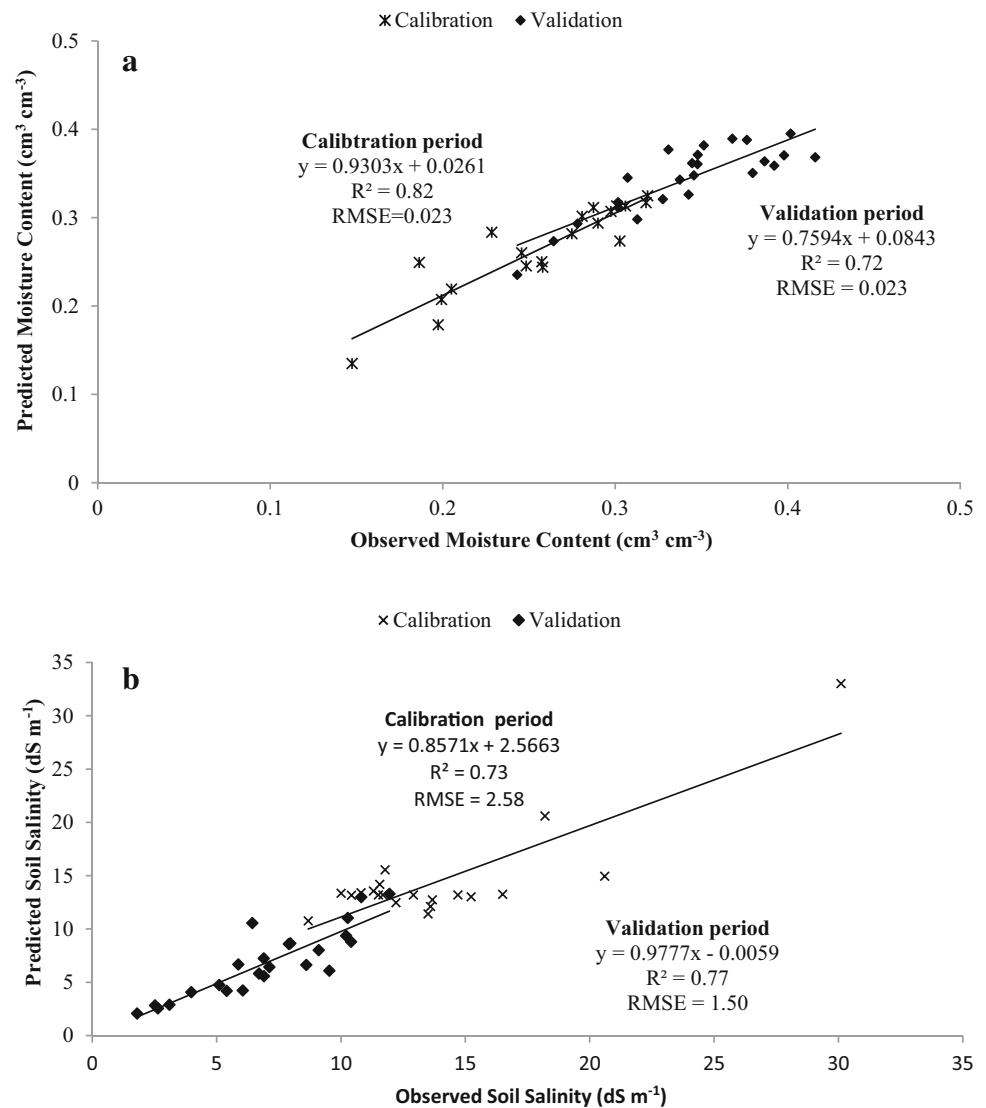
The Hydrus-1D model was calibrated using observed volumetric soil moisture content and soil salinity of 0–15, 15–30, 30–60 and 60–90 cm soil profile during 56–154 Julian days of the year 2015. For the calibration and validation of predictive models, statistical parameters such as coefficient of determination (R^2) and root mean square error (RMSE) were used (Fig. 4a, b). The calibrated hydraulic parameters for different depths are presented in Table 1 and these values were finally used for validation of

soil moisture and salinity data recorded for 197–288 Julian days of 2015.

Smaller $RMSE$ and higher R^2 values show that there was good agreement between the observed and simulated soil moisture contents and soil salinity (Fig. 4a, b). During calibration periods, $RMSE = 0.023 \text{ cm}^3 \cdot \text{cm}^{-3}$ and $R^2 = 0.82$ were observed for soil moisture content and $RMSE = 2.58 \text{ dS m}^{-1}$ and $R^2 = 0.73$ for soil salinity. Validation dataset resulted in $RMSE = 0.023 \text{ cm}^3 \cdot \text{cm}^{-3}$ and $R^2 = 0.72$ for soil moisture content and $RMSE = 1.5 \text{ dS} \cdot \text{m}^{-1}$ and $R^2 = 0.77$ for soil salinity.

These results revealed that although the model requires large input data, Hydrus-1D was an effective model for evaluating water and salute transport [18, 23] and would be effective in performing scenario simulations [6, 7] [2, 9, 29]. There is some difference observed between the simulated and measured soil water contents and soil

Fig. 4 a Observed and predicted soil moisture during calibration (56–154 Julian days, 2015) and validation period (197–288 Julian days, 2015). **b** Observed and predicted salinity during calibration (56–154 Julian days, 2015) and validation period (197–288 Julian days, 2015)



salinity. This difference probably due to preferential flow of water and solutes through macropores and cracks in the field condition [10], spatial heterogeneity and observation errors [27], adsorption–desorption and root uptake [11], and precipitation/dissolution reactions in soils [21]. Emphasizing Hydrus-1D as an effective model for evaluating soil moisture and salinity was also reported by several researchers [6, 7, 11, 12, 18]. The model prediction efficiency was higher for observed soil moisture content than for soil salinity. This may be attributed to the fact that model does not account for precipitation–dissolution reactions for solutes.

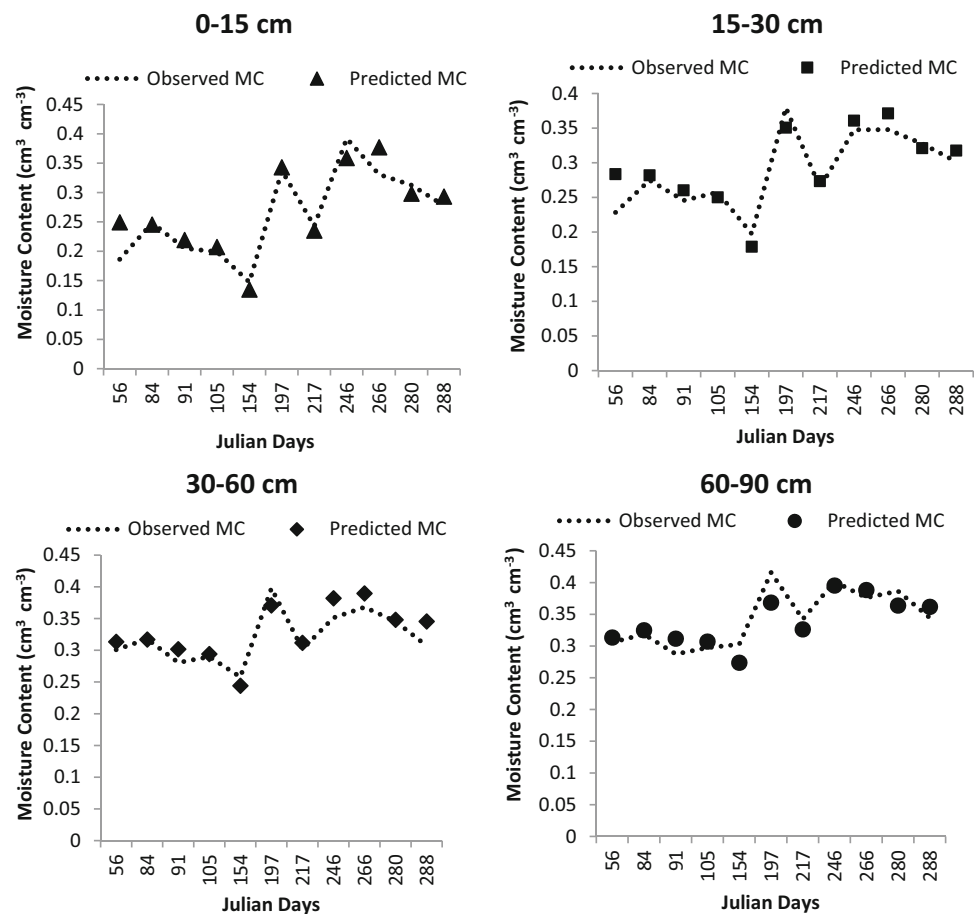
Soil Water and Salt Dynamics

Dynamics of profile water contents are primarily attributable to the rainfall, soil evaporation and depth to groundwater table (WTD). In general, soil moisture

contents increased depth-wise and were maximum in 60–90 cm soil layers (Fig. 5) probably due to the presence of shallow water table (0.87–3 m). The soil moisture at the 60–90 cm layer remained relatively constant during the growing season. In the surface soil layers (0–15 cm), soil moisture content fluctuated noticeably (0.15–0.36 cm³ cm⁻³) mainly due to hot and dry weather during 54–154 Julian days (February–May) and thereafter monsoonal rainfall during 166–260 Julian days (June–September) (Fig. 5).

Similarly, due to hot and dry weather condition during 54–154 Julian days, soil evaporative demands were very high and soil salinity (EC_e) raises intensively with EC_e values increased from 10.77 to 33.3 dS m⁻¹ in the upper 0–15 cm surface soil layer (Fig. 6). However, high-intensity rainfall of 18.5 cm on 194 Julian days leached down salts and reduced the surface soil salinity from 33.3 to 2.55 dS m⁻¹. Similar trend was observed in 15–30 cm soil layer, although the magnitude

Fig. 5 Observed and simulated soil water contents at 0–15, 15–30, 30–60 and 60–90 cm depths estimated in Hydrus-1D during the calibration and validation periods



of EC_e ($15\text{--}21 \text{ dS m}^{-1}$) was lower than the surface (0–15 cm) soil layer. However, in the deeper soil layers (30–60 and 60–90 cm), shallow saline groundwater contribution to soil salinity was observed. In the sublayer (30–60) and subsoil layer (60–90), moderate ($6\text{--}16 \text{ dS m}^{-1}$) and minimal ($8\text{--}14 \text{ dS m}^{-1}$) fluctuation in soil salinity throughout the study period (1–288 Julian days) (Fig. 6) reflects the saline groundwater contribution to soil salinity build up.

Soil Salinity Dynamics (0–90 cm soil profile) Under Variable Shallow Groundwater Table Condition

The effect of different groundwater table depth conditions on soil salinity was not clearly visible during 1–90 Julian days of 2015 (Fig. 7). This was mainly because of low evaporative conditions prevails (0–2 mm evaporation per day) during that period. However, during summer season (March–May), the effects of WTD on soil salinity buildup were significantly observed. During the monsoon period of 160–230 Julian days (June–September), the root zone soil salinity was in a desalination phase in all water table depths scenarios, and the desalination was more profound in the deeper water table (Fig. 7). In 25% and 50% reduced WTD condition, average root zone soil salinity went below 4–5

dS m^{-1} , which is slightly or non-saline category (Fig. 7). In general, root zone soil salinity increased with rise in groundwater table, whereas the amplitude of the soil salinity decreased with the declining of groundwater table depth. Average root zone soil salinity increased by 6 and 12 dS m^{-1} when WTD raised by 25 and 50%, respectively, but negligible change in soil salinity was observed when groundwater table declined by 25 and 50% (Fig. 7). These results indicate that a shallow water table contributed to increased soil salinization. Working in similar direction, Sun et al. [25] reported that in shallow water table areas declining water table depth is an effective way to control soil salinization. Ibrakhimov et al. [8] found that shallow groundwater table depth resulted in increased soil salinization by annual addition of $3.5\text{--}14 \text{ t ha}^{-1}$ of salts. Wu et al. [28] reported that groundwater table depth plays a positive role in soil salinity transport. He further mentioned that with the declined WTD, the effect of WTD and groundwater salinity on soil salinity buildup decreases.

Effects of Reducing Evaporative Flux

The substantial effect of reducing evaporative flux on dynamics of soil salinity was considerably observed.

Fig. 6 Observed and simulated soil salinity (EC_e - $dS\ m^{-1}$) at 0–15, 15–30, 30–60 and 60–90 cm depths estimated in Hydrus-1D during the calibration and validation periods

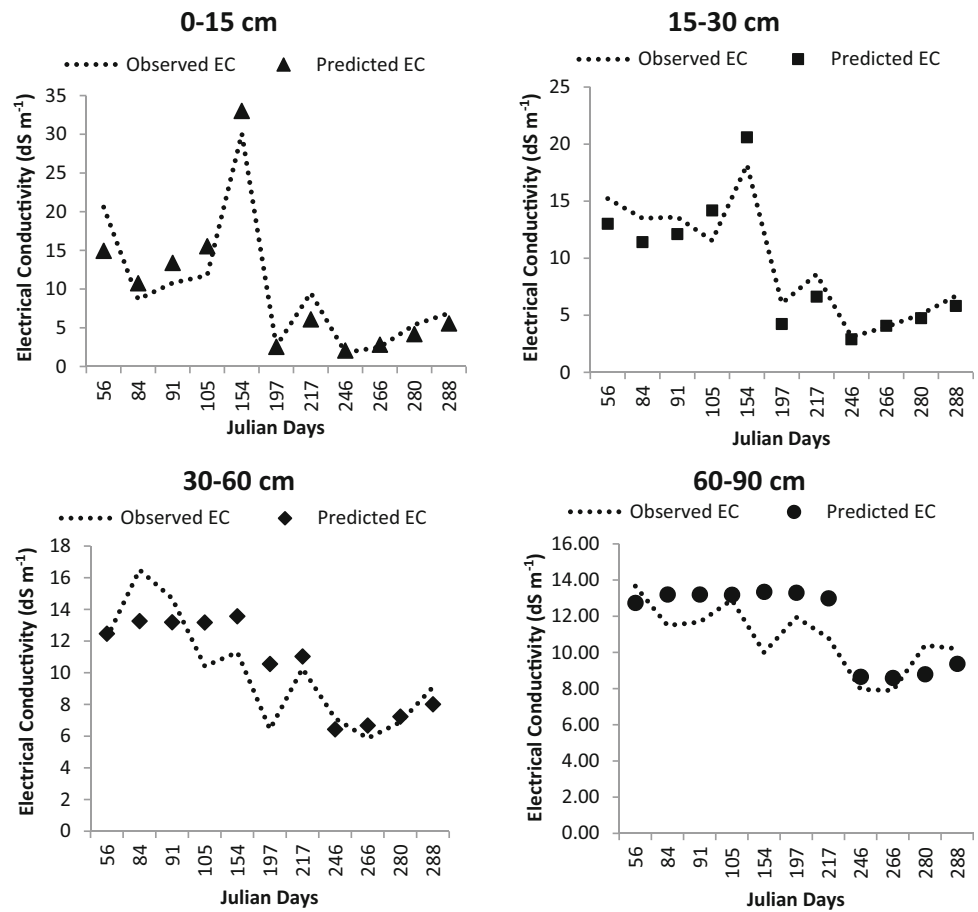


Fig. 7 Hydrus-1D simulated soil salinity dynamics (0-90 cm soil profile) under different water table depths

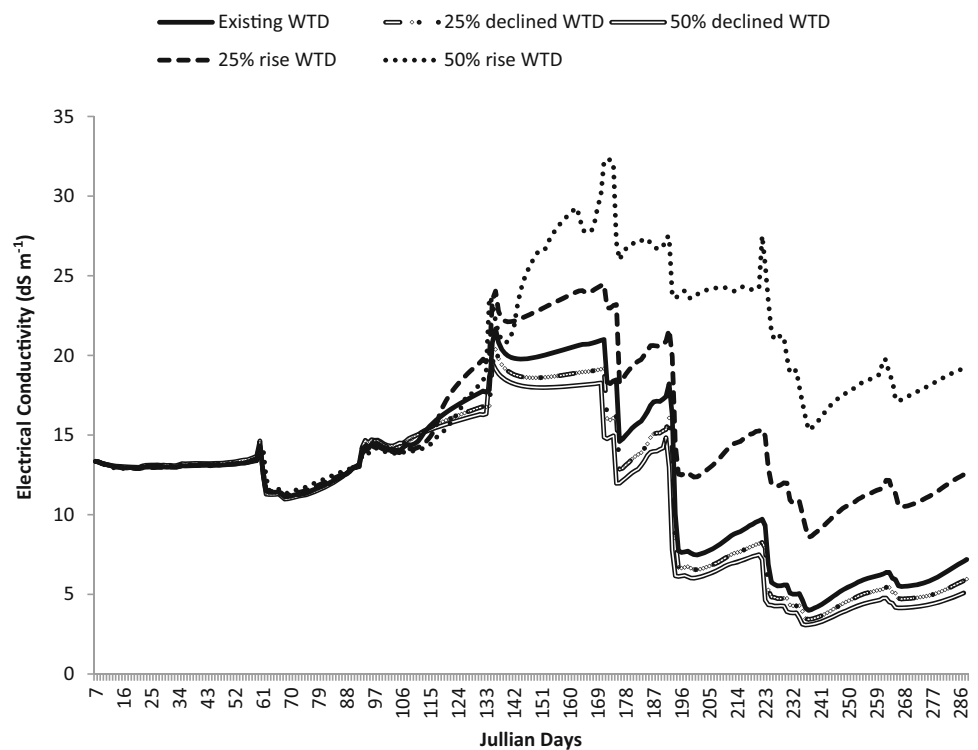
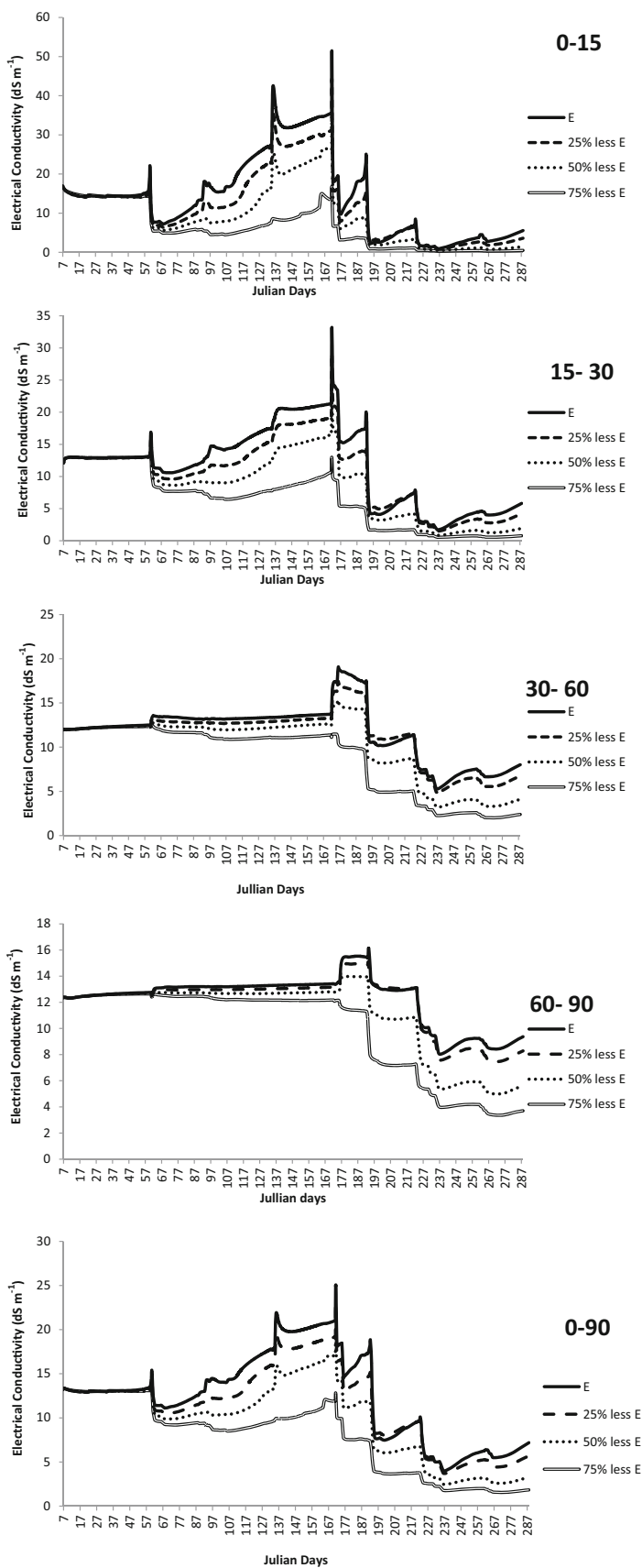


Fig. 8 Hydrus-1D simulated soil salinity dynamics under different evaporative condition 0–15, 15–30, 30–60, 60–90 and 0–90 cm soil profile depths



During summer season (50–154 Julian days), profile soil salinity (0–90 cm soil layer) ranges between 11.4 and 24.93 dS m⁻¹ with the actual evaporative flux (Fig. 8). However, for the same period, soil salinity under 25, 50 and 75% reduced evaporative flux ranges between 10.78 to 21.4 dS m⁻¹, 10.22 to 17.95 dS m⁻¹ and 9.65 to 12.55 dS m⁻¹, respectively. This was due to fact that during summer season capillary rise from the shallow saline groundwater was reduced with the decreasing evaporative flux resulted in less transportation of salts. The effect of this reducing evaporative flux was even more pronounced when focusing on the upper 0–15 and 15–30 cm of soil profile compared to sub (30–60 cm) and subsoil (60–90 cm) layer profile. In surface (0–15 cm) layer, maximum soil salinity (51.48 dS m⁻¹) was projected in actual evaporative flux in 154th Julian day (Fig. 8), while, with 25% reduced evaporative flux, projected surface maximum soil salinity was 43.52 dS m⁻¹. Further, in 50 and 75% reduced evaporative flux condition, projected maximum soil salinity was 35.17 and 16.03 dS m⁻¹. Although same trend was observed for the 15–30 cm soil layer, but magnitude of salinity was less than the surface layer. Soil salinity decreased in the monsoon season (154–260 Julian days) and profile soil salinity during these period ranges between 1.7 and 4.2 dS m⁻¹, maximum (4.2 dS m⁻¹) in the actual evaporative condition and minimum in 75% reduced evaporative condition (1.7 dS m⁻¹) (Fig. 8). Profile salinity reduction through crop residues retention was also reported by Forkutsa et al. [6, 7]; Devkota et al. [3]. Based on simulation study with Hydrus-1D, Forkutsa et al. [6, 7] reported that profile salt content reduced by 19% when evaporative flux was reduced by 50% through surface residue layer as compared to residue-free conditions. Devkota et al [3] observed that the soil salinity under permanent bed with residue was reduced by 22% over the top 90 cm soil profile compared to conventional tillage without crop residue retention. The benefits of reducing evaporative flux through a surface residue layer not only help to minimize soil salinization but also help to conserved soil moisture in turn means that less water is needed for pre-season salt leaching and improved crop germination.

Conclusion

Shallow saline groundwater plays an important role in soil salinization. Due to limited availability of land and water in semiarid region, it is important to manage shallow saline groundwater to prevent the land from salinization. To develop strategies for managing soil salinity, simulation studies were performed with numerical water and solute transport model Hydrus-1D. The Hydrus-1D model was found useful for simulations of soil water and salt dynamics as observed and simulated data fairly well during

both the calibration and validation periods. Simulation results indicated that summer season (March to May, 60–150 Julian days) is the most important time to control soil salinity. Considerable upward salt movement occurred during this period with 25 and 50% rise in groundwater table depth. The effective way to control this upward salt movement was reducing evaporative demands. Simulation study indicated that reducing evaporative flux by 25, 50 and 75% reduced profile soil salinity by 3.53, 6.95 and 12.38 dS m⁻¹, respectively, during peak summer period. From the results of the study, we can draw inference that declining water table depth and reduced evaporative losses can alleviate the problem of soil salinity and these are the effective and practical way to control soil salinity.

Acknowledgement The authors are thankful to Director ICAR-Central Soil Salinity Research Institute (Research Article/122/2020) for providing financial and logistic support toward execution of research work. Authors are also grateful to the Head, Division of Irrigation and Drainage Engineering, ICAR-Central Soil Salinity Research Institute, Karnal, for extending his technical and logistics support during execution of this study.

Compliance with Ethical Standards

Conflict of interest It is declared that authors do not have any conflict of interest in this publication.

References

1. Bezborodov GA, Shadmanov DK, Mirhashimov RT, Yuldashev T, Qureshi AS, Noble AD, Qadir M (2010) Mulching and water quality effects on soil salinity and sodicity dynamics and cotton productivity in Central Asia. *Agricul Eco Environ* 138:95–102
2. Dash CJ, Sarangi A, Singh DK, Singh AK, Adhikary PP (2015) Prediction of root zone water and nitrogen balance in an irrigated rice field using a simulation model. *Paddy Water Environ*, 13:281–290
3. Devkota M, Martius C, Gupta RK, Devkota KP, McDonald AJ, Lamers JPA (2015) Managing soil salinity with permanent bed planting in irrigated production systems in Central Asia. *Agric Ecosys Environ* 202:90–97
4. Dong HZ, Li WJ, Tang W, Zhang DM (2008) Furrow seeding with plastic mulching increase stand establishment and lint yield of cotton in a saline field. *Agron Jou*. 100:1640–1646
5. Egamberdiev O (2007) Dynamics of irrigated alluvial meadow soil properties under the influence of resource saving and soil protective technologies in the Khorezm region. Dissertation National University of Uzbekistan, p 123
6. Forkutsa I, Sommer R, Shirokova YI, Lamers JP, Kienzler K, Tischbein B, Martius C, Vlek PLG (2009) Modeling irrigated cotton with shallow groundwater in the Aral Sea Basin of Uzbekistan: I. Water dynamics. *Irriga Sci* 27:331–346
7. Forkutsa I, Sommer R, Shirokova YI, Lamers JP, Kienzler K, Tischbein B, Martius C, Vlek PLG (2009) Modeling irrigated cotton with shallow groundwater in the Aral Sea Basin of Uzbekistan: II. Soil salinity dynamics. *Irriga Sci* 27:319–330
8. Ibrakhimov M, Khamzina A, Forkutsa I, Paluasheva G, Lamers JPA, Tischbein B, Vlek PLG, Martius C (2007) Groundwater table and salinity: spatial and temporal distribution and influence

- on soil salinization in Khorezm region (Uzbekistan, Aral Sea Basin). *Irriga Drainage Syst* 21:219–236
9. Karimov AK, Šimunek J, Hanjra MA, Avliyakov M, Forkutsa I (2014) Effects of the shallow water table on water use of winter wheat and ecosystem health: implications for unlocking the potential of groundwater in the Fergana valley (Central Asia). *Agric Water Manage* 131:57–69
 10. Garg KK, Das BS, Safeeq M, Bhadoria PBS (2009) Measurement and modeling of soil water regime in a lowland paddy field showing preferential transport. *Agric Water Manag* 96(12):1705–1714
 11. Li H, Yi J, Zhang J, Zhao Y, Si B, Hill LR, Cui L, Liu X (2015) Modeling of soil water and salt dynamics and its effects on root water uptake in Heihe Arid Wetland, Gansu, China. *Water* 7:2382–2401
 12. Lyu S, Chen W, Wen X, Chang AC (2019) Integration of HYDRUS-1D and MODFLOW for evaluating the dynamics of salts and nitrogen in groundwater under long-term reclaimed water irrigation. *Irriga Sci* 37:35–47
 13. Mandal AK, Sethi M, Yaduvanshi NPS, Yadav RK, Bundela DS, Chaudhari SK, Chinchmalatpure A, Sharma DK (2013) Salt affected soils of nain experimental farm: site characteristics, reclaimability and potential use. *Technical Bulletin: CSSRI/Karnal/2013/03*, pp-34
 14. Mandal AK, Sharma RC, Singh G (2009) Assessment of salt affected soils in India using GIS. *Geocarto Int* 24:437–456
 15. Minhas PS, Ramos TB, Ben-Gal A, Pereira LS (2020) Coping with salinity in irrigated agriculture: crop evapotranspiration and water management issues. *Agric Water Manage* 227:105832. <https://doi.org/10.1016/j.agwat.2019.105832>
 16. Narjary B, Meena MD, Kumar S, Kamra SK, Sharma DK, Triantafyllis J (2019) Digital mapping of soil salinity at various depths using an EM38. *Soil Use Manage*. 35:232–244
 17. Pang HC, Li YY, Yang JS, Liang YS (2009) Effect of brackish water irrigation and straw mulching on soil salinity and crop yields under monsoonal climatic conditions. *Agric Water Manage* 97:1971–1977
 18. Ramos TB, Šimunek J, Goncalves MC, Martins JC, Prazeres A, Castanheira NL, Pereira LS (2011) Field evaluation of a multi component solute transport model in soils irrigated with saline waters. *J Hydrol* 407:129–144
 19. Rhoades JD (1999) Use of saline drainage water for irrigation. In: Skaggs RW, van Schilfgaarde J (eds) *Agricultural drainage American society of agronomy (ASA)–crop science society of America (CSSA)–soil science society of America (SSSA)*, Madison, Wisconsin, USA, pp 615–657
 20. Rhoades JD, Bingham FT, Letey J, Hoffman GJ, Dedrick AR, Pinter PJ, Replogle JA (1989) Use of saline drainage water for irrigation: imperial valley study. *Agric Water Manage* 16:25–36
 21. Rhoades JD, Chanduvi F, Lesch S (1999) *Soil salinity assessment: methods and interpretation of electrical conductivity measurements*, vol 57. Food and Agriculture Organization of the United Nations, Italy
 22. Rhoades JD, Kandiah A, Mashali AM (1992) *The use of saline waters for crop production-FAO irrigation and drainage paper no 48*. FAO, Rome
 23. Satpute ST, Singh M (2017) Potassium and sulfur dynamics under surface drip fertigated onion crop. *J Soil Salini Water Quali* 9:226–236
 24. Šimunek J, van-Genuchten MT, Sejna M (2005) The hydrus-1d software package for simulating the one-dimensional movement of water, heat, and multiple solutes in variably-saturated media. *Univ Calif Riverside Res* 3:1–240
 25. Sun G, Zhu Y, Ye M, Yang J, Qu Z, Mao W, Wu J (2019) Development and application of long-term root zone salt balance model for predicting soil salinity in arid shallow water table area. *Agric Water Manage* 213:486–498
 26. Tyagi NK (1998) Improvement in irrigation system for salinity control. In: Tyagi NK and Minhas PS (eds) *Agriculture salinity management in India*. Central Soil Salinity Research Institute, India, pp 309–324
 27. Vazifedoust M, van Dam JC, Feddes RA, Feizi M (2008) Increasing water productivity of irrigated crops under limited water supply at field scale. *Agric Water Manag* 95(2):89–102
 28. Wu X, Xia J, Zhan C, Jia R, Li Y, Qiao Y, Zou L (2019) Modeling soil salinization at the downstream of a lowland reservoir. *Hydrol Res* 50(5):1202–1205. <https://doi.org/10.2166/nh.2019.041>
 29. Xie T, Liu X, Sun T (2011) The effects of groundwater table and flood irrigation strategies on soil water and salt dynamics and reed water use in the Yellow River Delta China. *Ecol Model* 222:241–252
 30. Yuan C, Feng S, Huo Z, Ji Q (2019) Effects of deficit irrigation with saline water on soil water-salt distribution and water use efficiency of maize for seed production in arid Northwest China. *Agric Water Manage* 212:424–432
 31. Zhu Y, Ren L, Horton R, Lü H, Wang Z, Yuan F (2017) Estimating the contribution of groundwater to the root zone of winter wheat using root density distribution functions. *Vadose Zone J* 17:170075. <https://doi.org/10.2136/vzj2017.04.0075>

Publisher's Note Springer Nature remains neutral with regard to jurisdictional claims in published maps and institutional affiliations.